

RESEARCH ARTICLE

Communication Assisted Protection Scheme Based on Artificial Neural Networks for Multi-Microgrid

ALI F. QUSAYER¹ AND S. M. SUHAIL HUSSAIN^{1,2}, (Senior Member, IEEE)

¹Electrical Engineering Department, King Fahd University of Petroleum and Minerals (KFUPM), Dhahran 31261, Saudi Arabia

²Interdisciplinary Research Center for Sustainable Energy Systems (IRC-SES), King Fahd University of Petroleum and Minerals (KFUPM), Dhahran 31261, Saudi Arabia

Corresponding author: S. M. Suhail Hussain (suhail@ieee.org)


The authors would like to express their profound gratitude to King Abdullah City for Atomic and Renewable Energy (K.A.CARE) for their financial support in accomplishing this work.

ABSTRACT Designing a properly coordinated protection scheme for a multi-microgrid is very challenging because of their distinct characteristics. A microgrid can be operated in a grid-connected mode through direct connection to utility or through another grid-connected microgrid. It can also operate in an islanded mode or get connected with another independent microgrid. The various operation modes and topologies under which the system may operate bring major challenges such as the bi-directional flow of power and substantial variation in fault current. Such characteristics make protection schemes of conventional radial distribution systems unreliable options. In this paper, a centralized communication-assisted protection scheme based on artificial neural networks is proposed. The scheme operates in a cascaded process. In the first stage, a central protection controller is responsible of identifying and isolating the microgrid or tie line which has the fault. In the second stage, the local protection controller will be activated due to detection of islanding condition. It will then identify and isolate the faulty line accordingly. Identification of fault location is accomplished through neural networks trained with massive amount of three phase voltage and current measurements of all buses and lines during different fault scenarios using MATLAB/Simulink environment. The proposed scheme utilizes IEC 61850 based standardized communication to monitor the multi-microgrid and send the trip commands. Finally, the performance evaluation of the proposed scheme in terms of end-to-end delays including neural networks computational delay and communication network delay through extensive simulations is also presented which proves the effectiveness of the proposed protection scheme.

INDEX TERMS Communication assisted protection, distributed energy resources, microgrid, neural networks.

I. INTRODUCTION

Due to the arising concerns related to global warming, environmental pollution and resource limitation associated with fossil sources, the world is moving towards the utilization of alternative clean and sustainable energy sources. The introduction of smart grid has helped in the integration of these environment friendly renewable energy resources. Where conventional electric grids deliver electricity from

The associate editor coordinating the review of this manuscript and approving it for publication was Padmanabh Thakur .

power sources such as nuclear, coal, hydel and gas plants to consumers directly, the new generation electric grids i.e., “smart grids” have been introduced to reverse this transaction, permitting bidirectional flow of energy. Today’s power networks contain a utility grid (main grid) connected to many microgrids distributed at consumers locations.

Microgrids can be considered small versions of conventional utility grids functioning either independently or with interconnection to the main grid. Reliable and efficient microgrid operation relies primarily on the connected distributed energy resources (DERs). Wind turbines, PV systems, fuel

cells, diesel generators and energy storage systems are various examples of DERs [1], [2]. Recently, the concept of microgrid has evolved into multi-microgrid or networked microgrids to overcome the limitations related to the size and capacity of single microgrids. The evolution of multi-microgrids will enable better realization of the benefits associated with renewable energy integration [3].

Due to this change in the power network structure and other reasons which will be explored later, traditional protection systems used for conventional electric grids cannot be used to effectively protect single or multi-microgrids. In other words, using conventional protection schemes especially those suitable for radial systems results in very low dependability which make them inappropriate for modern meshed distribution systems with DERs. Accordingly, it became significantly important to come up with alternative protection designs to allow for safe and reliable integration between the main grid and microgrids. Indeed, it would be preferable from economical point of view to develop solutions making use of existing protection systems through some sorts of modifications or upgrade to meet the needs of microgrid protection instead of discarding the old system and installing a completely new protection system. Such approach is very expensive and not recommended. Therefore, a lot of research has been conducted in this area to identify ways of effective utilization of the existing conventional protection systems infrastructures of distribution systems [1].

There are several challenges which make conventional protection systems ineffective for use in microgrids. One main challenge is the significant variation of short circuit level in the microgrid as it can operate in grid-connected or islanded modes. In the normal operation mode, both the utility grid and distributed energy resources (DERs) contribute to the fault current during fault conditions. On the other hand, only the DERs supply fault current in the islanded mode. Accordingly, the short circuit level in the islanded mode is significantly lower than that of the grid connected mode. Therefore, microgrid protection design should take into consideration this variation in fault current to act properly in all expected faults scenarios [4].

Another major challenge is the bidirectional flow of power. In microgrids feeders, power can flow in the two directions due the changes in the amount of power generated and consumed within the microgrid which will be translated into either exporting or importing power from the utility grid. Such changes in the direction of power flow results in relay coordination problems leading to undesired tripping during fault conditions. This is another issue which should be considered for microgrid protection design [5].

In this paper, a communication-assisted protection scheme based on artificial neural networks (ANN) is proposed to overcome these challenges. The scheme works in two stages. In the first stage, identification and isolation of the microgrid or tie line which has the fault are achieved by the central protection controller. Then, the local protection controller will be activated in the second stage due to detection of islanding

condition. The local controller is responsible of identifying and isolating the faulty line. The process of faults detection and localization is accomplished through artificial neural networks. Using MATLAB/Simulink environment, these neural networks are trained with huge amount of three phase voltage and current measurements of all buses and lines during different fault scenarios. In addition, IEC 61850 based standardized communication is utilized to monitor the multi-microgrid and send the trip commands. Performance evaluation of the proposed scheme in terms of end-to-end delays is also included in this work. This end-to-end delay includes neural networks computational delay and communication network delay calculated through extensive simulations to prove the effectiveness of the proposed protection scheme.

The rest of the paper is organized as follows. The next section is a literature review. The third section presents the proposed communication assisted protection strategy. The test system is presented in the fourth section whereas the results are discussed in the fifth section. In the sixth section, the conclusion is presented. Future work is proposed in the last section.

II. LITERATUR REVIEW

Several protection techniques have been introduced to address the issues encountered with microgrid protection design. A literature survey in this regard is presented below.

Reference [6] proposes a differential protection scheme with two differential relays located on both sides of the protected power line. A communication link exists between the two relays to exchange currents measurements. Each relay is responsible for tripping the circuit breaker at its local end. The relays are equipped with three elements for phase differential currents to act promptly on faults having high currents. Two other differential elements for negative and zero sequence currents are also available for unbalanced high impedance faults which have low fault currents. In case of communication failure, overcurrent protection will be online as the first backup protection scheme. However, since overcurrent relays may not sense the low fault currents in the islanded mode of operation, undervoltage protection is deployed as a second backup protection. The two backup schemes are blocked whenever differential protection is in normal condition.

Authors in [7] proposes a novel solution for protecting microgrids with inverter based DER's using adjustable differential protection based on positive sequence currents. The reason for selecting positive sequence current instead of phase currents is to optimize the utilization of communication channels. In addition, since positive sequence current is present in all faults scenarios which is not the case for negative sequence and zero sequence currents, it can be used to detect all types of faults i.e., single line to ground, line to line, double line to ground and three phase faults. Two settings are available for the proposed differential protection scheme according to the mode of operation (grid connected or islanded). The scheme starts with detecting an abnormal condition through undervoltage detection since faults result

in voltage sags. Then, the current magnitude at each side of the power line is inputted to comparators to reveal the microgrid mode of operation. In grid-connected operation, the fault current magnitude is normally higher than the magnitude of fault current in islanded mode of operation. Then, based on the detected mode of operation the differential positive sequence current is compared with one of the two settings to take the needed action. In [8], a protection scheme based on nonstandard characteristics curves for overcurrent relays was proposed using a logarithmic function and variable coefficient. The scheme uses two optimization techniques which are genetic algorithm and a hybrid technique combining gravitational search algorithm and sequential quadratic programming. The scheme was implemented on IEC MG, IEEE 9-bus and IEEE 30-bus systems successfully.

The authors of [9] suggests the utilization of fault current limiter (FCL) to accurately estimate the fault current in a microgrid with inverter-interfaced distributed generators (IIDG's). Each IIDG is equipped with an FCL limiting the output current of the DG during fault conditions to a predetermined value. Such configuration enables exact knowledge of fault currents instead of approximation which will enhance the performance of the overall protection system. A Central Protection Unit (CPU) is required to continuously monitor the DG's statuses through communication links. Whenever a DG is connected or disconnected, the CPU re-calculates the fault currents and update the relays' settings of the microgrid accordingly. To optimize the connections required in this communication assisted protection scheme, the CPU may rely on the relays connected to the DGs to get their statuses. In this way, the communication links between the CPU and the DG's can be omitted.

Reference [10] applied optimization algorithms to size the FCL impedance for minimizing the variation of microgrid fault currents. In their study, FCLs were placed in series with the DGs and the point of common coupling PCC. Then, the impedance matrices of the microgrid were established for three different configurations (grid-connected with/without DGs and islanded mode of operation). After that, FCL sizes were selected to minimize the differences between the three configurations. Finally, they succeeded to reduce the fault current variation in the three configurations from 5 kA to less than 0.5 kA.

To support the recognition of microgrid topology, a machine learning technique using artificial neural networks ANN is proposed in [11]. The ANN is trained with massive simulation or real data to identify whether a fault is present in the microgrid and which feeder is faulty based on voltage and current measurements of all buses. The logic is triggered by the detection of a tripping signal. Then, the tripped feeder will be restored if the ANN concludes no fault condition in the microgrid which is the case for intermittent faults. If a permanent fault is present, the ANN will identify the faulty line. Then, decision tables will be retrieved to execute any changes required on protective relay settings.

Another application for artificial intelligence was presented in [12] where convolutional neural networks CNNs were used to identify fault type, phase and location for proper fault isolation and recovery. Three independent CNNs were developed to cover these three functions. The three phase currents sampled by the relay were used as inputs to the CNN's. Then, training and testing data were generated through simulation in MATLAB/Simulink where various scenarios were considered such as changes in microgrid operation modes, topology, different fault types, resistances and locations. Indeed, the testing results showed high accuracy for the designed CNNs. Such solution will help reducing the dependency on communication links which is the major drawback of adaptive protection.

However, the effectiveness of the abovementioned protection schemes cannot be generalized on a multi-microgrid system which has a wider range of short circuit current variation. Further evaluation is still required.

In [13], a communication-based adaptive protection scheme is proposed for a multi-microgrid system based on IEC 61850 communication protocol. The microgrid management system detects the topology of the microgrids system by analyzing the breakers status received through generic object-oriented substation events (GOOSE) messages. Accordingly, it will instruct the intelligent electronic devices (IEDs) to enable the adequate set of trip settings. GOOSE messages are also exchanged among the IEDs to identify the direction and location of the fault current to take the necessary action. The scheme was verified through artificial faults applied in the testing microgrid of the Institute of Nuclear Energy Research, Taiwan.

Another communication-based adaptive protection scheme was proposed by the authors of [14]. However, this scheme works in a decentralized manner where adaptive overcurrent IEDs respond to the faults through two settings groups corresponding to the islanded and grid-connected modes of operation. Setting groups are updated using the status signals of circuit breakers received through GOOSE messages. In addition, these IED's take trip decisions based on information related to the status of circuit breakers, fault current detection and comparison of current magnitudes exchanged with other IEDs through GOOSE messages as well. The algorithm was implemented successfully in Power Systems Computer Aided Design (PSCAD).

Reference [15] extends adaptive protection application to a group of networked microgrids NMG specified in [16] using directional overcurrent relays DOCR's with multiple setting groups. Instead of recalculating the operating currents for every change in the NMG structure, selection from predetermined setting groups is employed. Changes in NMG structure take place when making or breaking connections among the microgrids and the utility grid. An NMG with 5 PCCs for example will result in $2^5 = 32$ topologies based on the different statuses of these PCC's. Optimization algorithms can be used to cluster these topologies into a certain number of

groups based on the capabilities of the DOCR's. For DOCR's with 8 setting groups, the NMG topologies can be clustered in 8 groups. Topologies with fault currents falling in the same range can be put in one group. Then, optimum operating currents and time delays are calculated for each relay and should be active for all topologies in that particular group. The NMG Energy Management System EMS monitors changes in the NMG topologies and send signals to enable the proper setting group for each relay as required through low bandwidth communication links. However, this scheme does not assure minimum operating time for the relays in each topology due to the restrictions associated with the limited number of setting groups. Reference [17] proposes adaptive protection scheme using digital DOCRs accepting on-line update of relay settings. Updated settings are calculated using Interior Point Optimization technique based on real-time status of the system obtained through communication channels and intelligent electronic devices. The scheme was tested on a standard IEEE 14-bus distribution system with consideration of a distributed generator.

In light of the literature review presented above, several gaps can be recorded against the available solutions for MMG protection. Firstly, most of the protection solutions proposed in the literature were developed for single MGs. The effectiveness of these protection schemes cannot be directly generalized to MMGs which have a wider range of short circuit current variation and a huge number of possible network configurations. Further evaluation is still required.

Regarding protection solutions based on machine learning, the protection schemes proposed in the literature focused mainly on faults detection and classification. Only limited number of publications presented a complete protection scheme covering all stages from fault detection to fault clearance.

Moreover, the performance of communication-assisted protection solutions available in the literature was mostly evaluated from the perspective of protection scheme functionality only. However, the feasibility of the solution from communication network side was not considered. To ensure comprehensive evaluation, the communication network for such solutions should be designed and the communication delays should be analyzed.

In this paper, a communication-assisted ANN-based protection strategy is proposed for MMG protection to fill the identified research gaps. The strategy is tested on a modified IEEE 14-bus distribution system.

III. PROPOSED COMMUNICATION ASSISTED PROTECTION STRATEGY

This article proposes a centralized communication-assisted ANN-based protection scheme for MMG. The proposed scheme is operated in two stages. In the first stage, a central protection controller is responsible of identifying and isolating the MG or tie line which has the fault. If the fault is in a MG, the local protection controller will be activated due to detection of islanding condition. It will

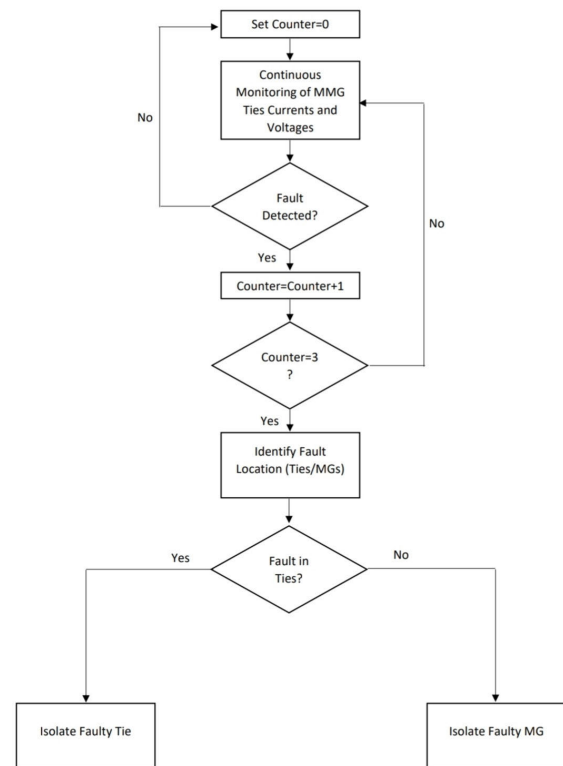


FIGURE 1. Proposed central MMG controller protection scheme.

then identify and isolate the faulty line accordingly. This scheme is demonstrated in Fig. 1 and 2. Counters were used in the scheme to ensure that trip decision is not taken based on a single set of measurements to avoid unnecessary trip by measurements errors. Identification of fault location is accomplished through ANNs trained with massive amount of three phase voltage and current measurements of all MMG buses and lines during different fault scenarios. Data generation and ANN training and testing are performed on MATLAB/Simulink environment. The proposed protective scheme ensures selective tripping which results in high level of power network availability. Moreover, the cascaded scheme will help optimize the size of the communication network due to reduction of required connections to the central controller. Indeed, it will also optimize the ANN design in terms of size, complexity and requirement for data generation to train the ANN. This in turn will speed up fault detection and location process.

One of the main characteristics of ANN is the ability to learn from examples and then generalize on a different set of data never seen before which makes it an excellent option for classification. This principle is used in the application of faults detection, classification and location. Based on a set of inputs which are the three-phase voltage and current measurements of the monitored buses and lines and a corresponding set of outputs which are the location and type of fault represented as a binary number, the ANN can extract

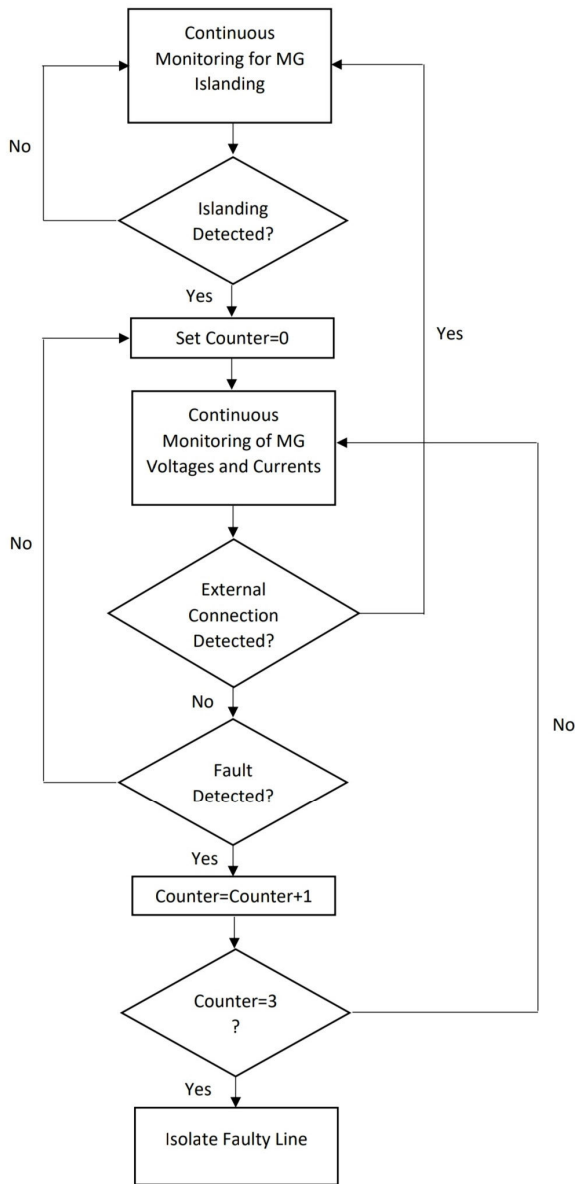


FIGURE 2. Proposed local MG controller protection scheme.

the relationship between these variables and make the generalization.

In this research, Levenberg-Marquardt backpropagation algorithm has been utilized for training the neural networks. This algorithm is a variant of the Gauss-Newton technique for solving nonlinear least-squares problems which can handle huge and complicated datasets and quickly converge to a solution [18]. It is an iterative technique that modifies the ANN weights to minimize the sum of squared errors between expected and actual output. The approach computes the gradient of the error function with respect to the ANN weights. The gradient is a vector that represents the direction in which the error function decreases the fastest. The algorithm then

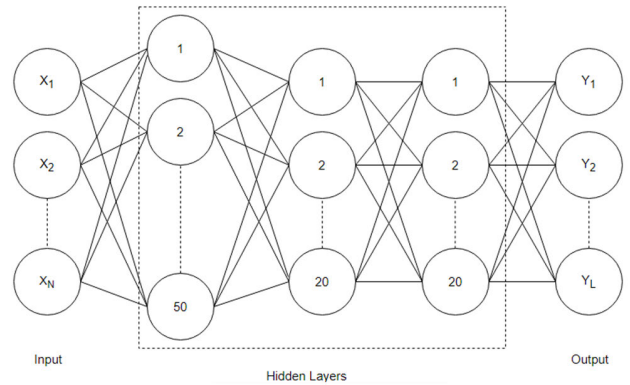


FIGURE 3. ANN topology.

adjusts the weights of the ANN in the direction of the negative gradient to minimize the error function [19].

A total of 196,066 and 282,914 patterns obtained through extensive MATLAB/Simulink simulations for various faults scenarios were used for training and testing the designed ANNs, respectively. Different MMG configurations, types of faults, fault resistances, distances, loading and generation conditions were applied to generate the data. Three different ANN topologies were used in this work based on the MMG configuration which controls the number of VI measurements in effect. For configurations resulting in less complicated classification problems, only one hidden layer with 20 or 30 neurons was utilized. However, for configurations with more complicated classification problems, three hidden layers of 50-20-20 neurons was utilized to achieve better performance as shown in Fig. 3. In this figure, the input layer of the neural network consists of the voltage and current measurements associated with each fault scenario. The output layer is the fault scenario represented as a binary number. For example, the output produced by the neural network in the first stage (central controller) is a ten-digit binary number of the sequence MG1-MG2-MG3-L6-L8-L14-A-B-C-G. In this output, “1” indicates “True” whereas “0” indicates “False”. If the output is “0001001001” for example, it means that Phase A-to-ground fault is present in line# 6.

IV. TEST SYSTEM

The proposed protection scheme has been tested on the modified IEEE-14 bus distribution system shown in Fig. 4 with the details given in Tables 1, 2 and 3. The synchronous generator short circuit level was considered five times its maximum generation limit [20]. On the other hand, the short circuit level of each wind turbine and photovoltaic system was considered as two and 1.5 times their maximum generation limits, respectively [21], [22].

In this research, simulation studies were performed in MATLAB R2023a [23], NetSim [24] and 61850 emulator tools [25] environments on a personal computer with Intel Core i7 processor and 16 GB RAM. Comprehensive

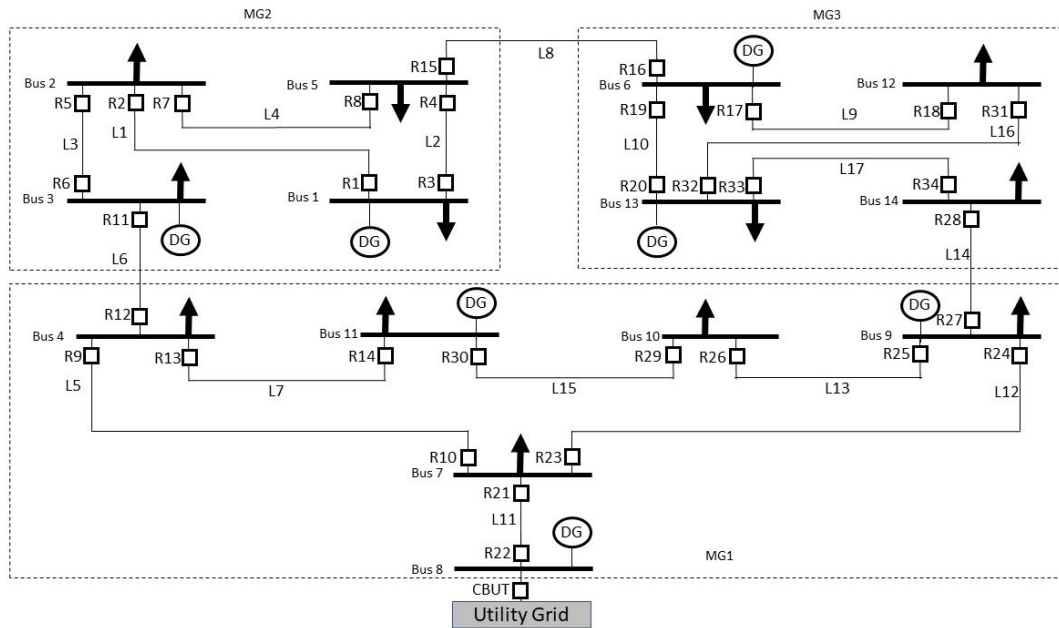


FIGURE 4. MMG test system (modified IEEE-14 bus system).

TABLE 1. MMG loads information.

Bus	P (kW)	Q (kVAR)	Bus	P (kW)	Q (kVAR)
1	580	150	8	--	--
2	439	135	9	500	45
3	673	96	10	637	33
4	439	135	11	788	95
5	600	128	12	125	50
6	560	112	13	169	20
7	851	145	14	200	43

TABLE 2. MMG generation information.

Bus	Generation Type	P (kW)	Qmin (kVAR)	Qmax (kVAR)	Short Circuit (kVA)
1	Photovoltaic	2000	0	500	3000
3	Photovoltaic	400	0	100	600
6	Photovoltaic	800	0	160	1200
8	Wind Turbine	800	-250	250	1600
9	Photovoltaic	800	0	160	1200
11	Synchronous Generator	2000	-1000	2000	10000
13	Photovoltaic	400	0	100	600
Utility	--	--	--	--	300000

performance evaluation of the proposed scheme is presented in the following section.

V. RESULTS AND DISCUSSION

A. FAULT DETECTION AND LOCALIZATION PERFORMANCE

As discussed earlier and shown in Fig. 1 and 2, the proposed protection scheme works in a cascaded process. The results of testing this scheme on the test MMG are summarized in this section. The central controller is responsible of isolating

TABLE 3. MMG lines information.

Line	Resistance (Ohm)	Reactance (Ohm)	Line	Resistance (Ohm)	Reactance (Ohm)
1	0.04668	0.05994	10	0.2226	0.1512
2	0.07002	0.08991	11	0.0309	0.0477
3	0.05835	0.07493	12	0.06224	0.07992
4	0.2226	0.1512	13	0.2226	0.1512
5	0.04668	0.05994	14	0.0309	0.0477
6	0.0309	0.0477	15	0.05835	0.07493
7	0.04668	0.05994	16	0.1908	0.1296
8	0.0309	0.0477	17	0.1908	0.1296
9	0.05446	0.06993			

the MG or tie line experiencing the fault condition. It will be enabled in all MMG configurations except when all the three MGs are islanded. Furthermore, the configurations are clustered into six groups. Each group corresponds to a certain ANN which the controller selects to monitor the condition of the MMG in order to detect and locate faults. The details of these groups and ANN performance are summarized in Table 4. Data was generated for training and testing the ANNs of the central protection controllers considering all possible types of faults, MMG topologies, different generation and loading conditions and typical fault resistances [26], [27].

Different ANN designs were tried for the purpose of detecting and locating faults within the MMG. The ANNs which produced the best training and testing performance were selected.

Similarly, simulation data was generated for training and testing the ANNs of the local protection controller of each MG. Different ANN topologies were tried for the purpose of detecting and locating faults within the MGs. The ANNs

TABLE 4. ANNs Performance for MMG Central Controller and MGs local controllers.

ANN	MMG Configuration				Training Patterns	Testing Patterns	Training Performance	Testing Performance	Computational Delay	Simulated Scenarios
	Utility	Line 6	Line 8	Line 14						
Central Controller Group 1	In	In	In	In	27,720	83,160	99.81%	99.21%	14 ms	Normal condition and all types of faults (ABC, AG, BG, CG, AB, BC, CA, ABG, BCG & CAG) in each line in all group topologies at 100% & 50% DER penetration, four loading conditions (25%, 50%, 75% & 100%), three different fault resistances (0.001, 10 & 50 Ohm) and three different distances along the lines (25%, 50% & 75%).
	In	In	In	Out						
	In	In	Out	In						
	In	Out	In	In						
	In	Out	In	Out						
	Out	In	In	In						
	Out	In	Out	In						
	Out	Out	In	In						
Central Controller Group 2	Out	Out	In	Out	5,400	1,800	99.44%	99.89%	10 ms	
Central Controller Group 3	In	Out	Out	In	12,960	4,320	100%	100%	20 ms	
	Out	Out	Out	In						
Central Controller Group 4	In	In	Out	Out	12,960	4,320	99.99%	100%	19 ms	
	Out	In	Out	Out						
Central Controller Group 5	In	Out	Out	Out	3,780	1,260	99.10%	100%	10 ms	
MG1 Controller	MG1 Islanded				53,866	161,594	99.97%	99.47%	8 ms	Normal condition and all types of faults (ABC, AG, BG, CG, AB, BC, CA, ABG, BCG & CAG) in each line in all possible combinations of lines and DERs availability at four loading conditions (25%, 50%, 75% & 100%), three different fault resistances (0.001, 10 & 50 Ohm) and three different distances along the lines (25%, 50% & 75%).
MG2 Controller	MG2 Islanded				38,070	12,690	99.36%	100%	8 ms	
MG3 Controller	MG3 Islanded				41,310	13,770	99.98%	100%	19 ms	

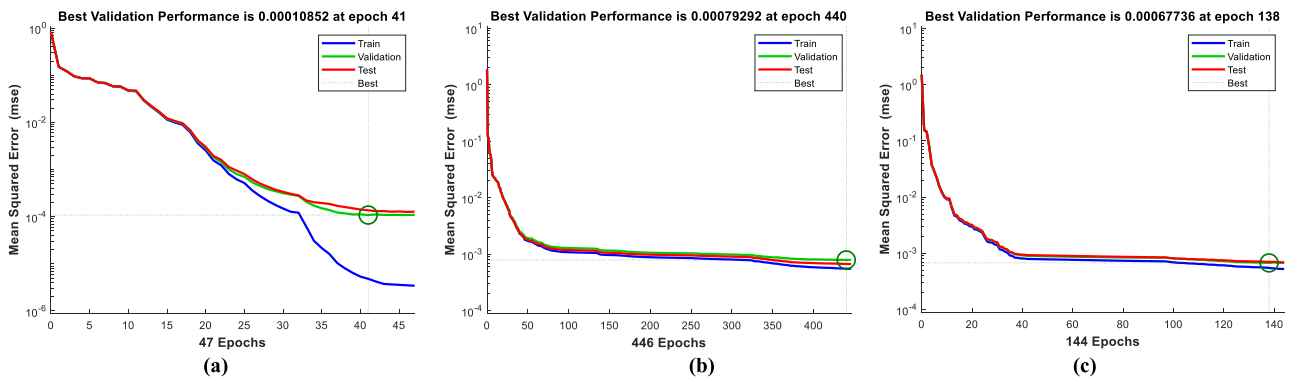


FIGURE 5. ANN training performance in terms of mean squared error (MSE) for (a) MG1 (b) MG2 and (c) MG3 controller.

TABLE 5. Fault classification accuracy of MGs neural network-based protection schemes.

Protection Scheme	[12]	Proposed
Total Patterns	11,402	196,066
Classification Accuracy	99.46%	99.74%

which produced the best training and testing performance were selected as demonstrated in Table 4. Figure 5 shows

the performance based on mean squared error (MSE) for the MG1, MG2 and MG3 controllers. It can be seen from Figure 5, best validation occurs at epoch 41, 440 and 138 for MG1, MG2 and MG3 controllers respectively. Finally, Figure 6 presents the regression plots which have coefficients very close to unity indicating excellent performance.

Although the neural networks-based protection schemes available in literature were developed mainly for single MGs

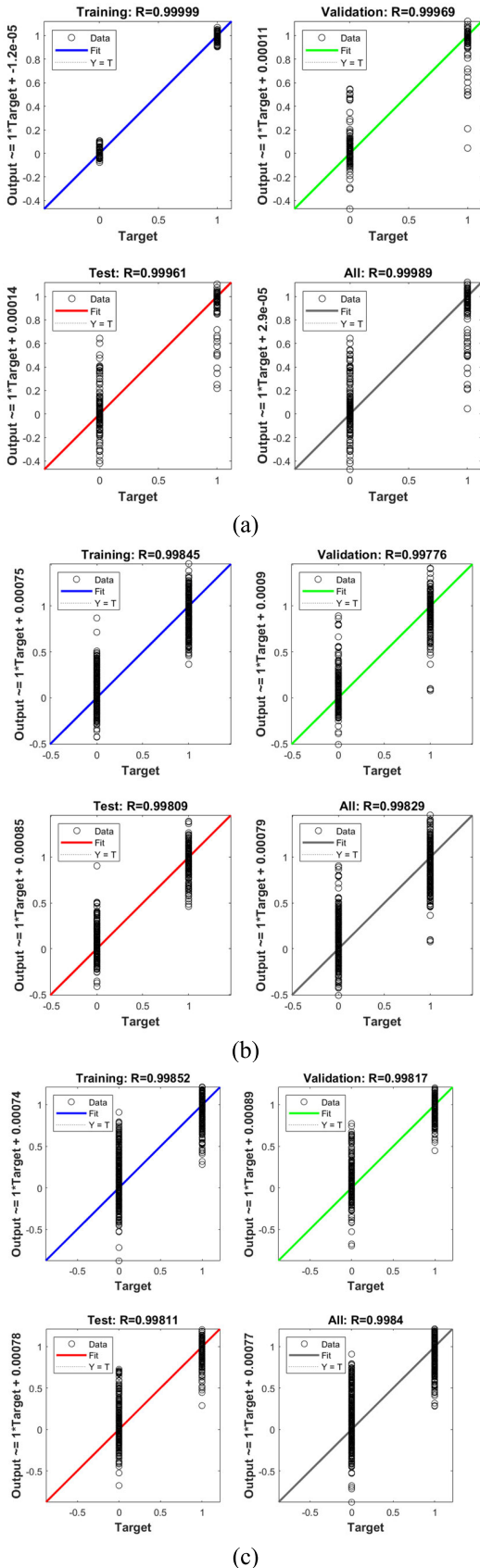


FIGURE 6. ANN regression for (a) MG1, (b) MG2 and (c) MG3 controllers.

and not for MMGs, they can still be compared with the protection scheme proposed in this paper from fault classification accuracy point of view. As can be seen from Table 5, the protection scheme proposed in this thesis outperforms other protection schemes available in literature in terms of MGs faults classification accuracy. One factor that led to such superiority is the extensive simulations performed to generate a huge amount of data for various fault scenarios which resulted in a very robust protection scheme.

B. COMMUNICATION DELAYS

The communication network of the MMG under study was simulated in NetSim environment. Each MG has a local protection controller and is supported by a dedicated local area network (LAN). The central protection controller is interconnected with the three local controllers through a network of four routers. Voltage and current measurements are transmitted over the network based on Routable Sampled Value (R-SV) protocol whereas breakers' status and trip commands are transmitted using Routable GOOSE (R-GOOSE) protocol [28]. Figure 7 shows the communication model of the test MMG simulated in NetSim. For each bus, one node was used to represent the merging unit (MU) IED responsible of sharing the voltage measurements. For each line, two nodes were used to represent the MU IEDs at both ends to exchange the current measurements. A total of seven nodes were used to represent the Utility and tie line CBs to exchange the CB status. Other nodes were added to represent some breakers IEDs for simulating trip commands. The central and local protection controllers were also modeled as nodes interconnected with the remaining nodes through physical links, switches and routers. After building the model, various applications were defined for exchanging VI measurements, CB status and trip commands between the protection controllers, MUs and CB IEDs.

In order to calculate the realistic communication delays, we use a framework as shown in Fig. 8. First, realistic R-GOOSE and R-SV messages for the proposed scheme are generated using IEC 61850 emulator tools, then using Wireshark tool these messages are captured to determine its exact size. This size is then used in network simulator to model the R-GOOSE and R-SV traffic for the proposed protection scheme.

As an example, the Wireshark captured R-GOOSE messages published by local controller to trip breaker 80 and R-SV published by IED 49 updating its voltage and current measurements are illustrated in Fig's 9 and 10 respectively. The sizes of data packets identified using the discussed framework are 173 bytes for R-SV and 200 bytes for R-GOOSE. Sampling time of 4800/s was used for both measurements and breakers status.

The obtained message sizes and sampling times for all the R-GOOSE and R-SV message exchanges for the proposed protection scheme are set in NetSim simulation. The simulation shows that the communication delay using 100 Mbps

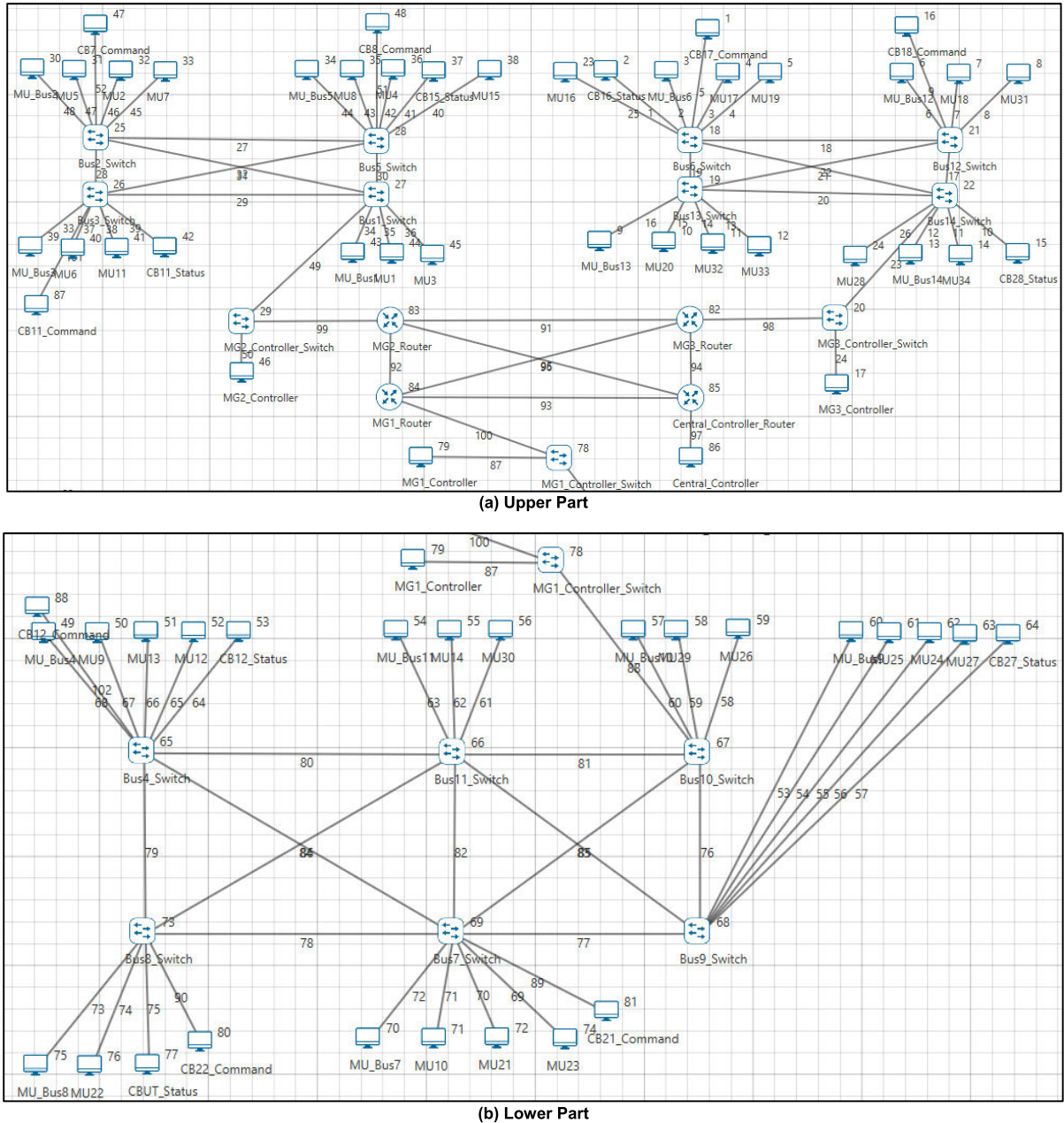


FIGURE 7. MMG communication network simulation.

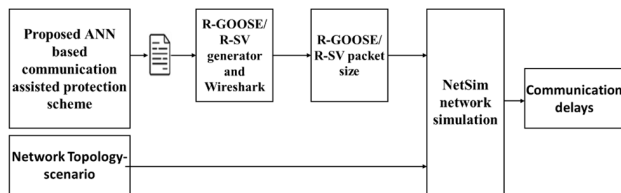


FIGURE 8. Framework for calculating realistic communication delays.

communication links is very huge reaching more than 1 s in some cases. To solve this issue, the communication links

capacity was increased to 1000 Mbps which resulted in delays not exceeding 130 microseconds (μ s). Some cases are demonstrated in Table 6.

C. END TO END DELAYS

Accordingly, the total end-to-end delays including both the communication network delay and ANN computational delay is dominated by the ANN computational delay. As shown in Table 4, the maximum computational delay is found to be 14 ms and the communication delays are in order of 100 micro seconds, which satisfies the 50 ms requirements for adaptive relaying as per the IEC 61850-90-5 standards.

TABLE 6. MMG communication delays.

Message #	Source	Destination	Parameter	100 Mbps Links		1000 Mbps Links	
				Delay (μs)	Jitter (μs)	Delay (μs)	Jitter (μs)
1	R9 MU*	MG1 Controller	VI Measurement	98777.28	9.796468	61.77686	0.02687
2	CB12	MG1 Controller	CB Status	97350.28	13.83665	79.06624	0.03787
3	MG1 Controller	CB21	Trip	83.9756	8.055517	65.66916	8.08613
4	R1 MU	MG2 Controller	VI Measurement	96867.75	11.58751	45.12169	0.00627
5	CB11	MG2 Controller	CB Status	83747.38	22.06389	79.06844	0.033
6	MG2 Controller	CB7	Trip	65.8936	0.915371	46.61557	0.39084
7	R17 MU	MG3 Controller	VI Measurement	96587.3	11.72656	48.32499	0.00611
8	CB28	MG3 Controller	CB Status	96570.31	11.71578	45.54992	0.00427
9	MG3 Controller	CB17	Trip	85.75898	0.167544	77.98448	0.26536
10	R11 MU	Central Controller	VI Measurement	1422297	189.3091	106.3407	0.10353
11	CB11	Central Controller	CB Status	1418837	188.9746	103.3832	0.09166
12	Central Controller	CB11	Trip	128.3195	0.168108	99.26626	0.26716

*Relay 9 MU

```

> Internet Protocol Version 4, Src: 172.24.14.26, Dst: 239.1.1.35
> User Datagram Protocol, Src Port: 57154, Dst Port: 102
> ISO 8602/X.234 CLTP ConnectionLess Transport Protocol
R-GOOSE
  > Session header
  > Session user information
    > Payload
      Payload length: 125
      Payload type tag: GOOSE (0x81)
      Simulation flag: 0x01 (1)
      APPID: 0x0001 (1)
      APDU length: 0x007b (123)
    > goosePdu
      gocbRef: LLN0$TripCB_Circuit_Breaker_80
      timeAllowedtoLive: 128
      datSet: LLN0$Circuit_Breaker_TripCB_80
      goID: CircuitBreaker80
      t: Nov 5, 2023 12:37:01.608999848 UTC
      stNum: 2
      sqNum: 6
      simulation: True
      confRev: 1
      ndsCom: False
      numDatSetEntries: 1
    > allData: 1 item
      > Data: boolean (3)
        boolean: True
    
```

```

0000  01 00 5e 01 01 23 f8 e4 3b e9 73 7b 08 00 45 e0  ..^..#.. ;s{
0010  00 ba e7 96 00 00 20 11 00 00 ac 18 0e 1a ef 01  ..I.....
0020  01 23 df 42 00 66 00 a6 ab 0e 01 40 a1 17 80 15  -#-B-f- ...@
0030  00 00 00 8d 00 00 00 1b 00 02 00 00 00 00 00 0a  .....
0040  00 00 00 01 00 00 00 00 7d 81 01 00 01 00 7b 61  .....}....
0050  77 80 1e 4c 4c 4e 30 24 54 72 69 70 43 42 5f 43  w-LLN0$ TripC
0060  69 72 63 75 69 74 5f 42 72 65 61 6b 65 72 5f 38  ircuit_B reake
0070  30 81 02 00 80 82 1e 4c 4c 4e 30 24 43 69 72 63  0-....-L LN0$C
0080  75 69 74 5f 42 72 65 61 6b 65 72 5f 54 72 69 70  uit_Brea ker_T
0090  43 42 5f 38 30 83 10 43 69 72 63 75 69 74 42 72  CB_80-C circui
00a0  65 61 6b 65 72 38 30 84 08 65 47 8c 6d 9b e7 6a  eaker80: eG-m
00b0  30 85 01 02 86 01 06 87 01 01 88 01 01 89 01 00  0-.....
00c0  R2 a1 a1 ah a2 a2 a1 a1 .....
    
```

FIGURE 9. R-GOOSE message Wireshark capture.

VI. CONCLUSION

In this paper, a centralized communication-assisted ANN-based protection scheme was proposed. The scheme operates in a two-stage process. Firstly, a central protection controller identifies and isolates the MG or tie line which has the fault. Then, the local protection controller is enabled once the islanding condition is detected. The local controller identifies and isolates the exact faulty line accordingly. Identification

```

> Frame 70: 173 bytes on wire (1384 bits), 173 bytes captured (1384 bits) on
> Ethernet II, Src: f8:e4:3b:e9:73:7b (f8:e4:3b:e9:73:7b), Dst: IPv4mcast_0
> Internet Protocol Version 4, Src: 172.24.14.26, Dst: 239.1.1.36
> User Datagram Protocol, Src Port: 58676, Dst Port: 102
> ISO 8602/X.234 CLTP ConnectionLess Transport Protocol
  > iec61850_90_5
    > SPDU type: 0xa2
    > Header
    > UserData
      > Payload
        User Data Type: SV
        Simulation Bit: TRUE
        Application ID: 16384
        Payload Length: 94
      > IEC 61850 SMV
        SMV 9-2
        Number of ASDUs: 1
        Start of ASDUs
          ASDU
            ID*: MU49
            Sample Count*: 0
            Config Rev*: 1
            Sample Synced: not synced (0)
            Samples:
              ImATCTRL1.Amp.instMag.i: 0
              ImATCTRL1.Amp.q: validity = good Process Measured
              ImBTCTRL2.Amp.instMag.i: 86603
              ImBTCTRL2.Amp.q: validity = good Process Measured
              ImCTCTRL3.Amp.instMag.i: -86603
              ImCTCTRL3.Amp.q: validity = good Process Measured
              ImNmCTRL4.Amp.instMag.i: 0
              ImNmCTRL4.Amp.q: validity = good Process Measured
              UmnATVTR1.Vol.instMag.i: 0
              UmnATVTR1.Vol.q: validity = good Process Measured
              UmnBTVTR2.Vol.instMag.i: 86603
              UmnBTVTR2.Vol.q: validity = good Process Measured
              UmnCTVTR3.Vol.instMag.i: -86603
              UmnCTVTR3.Vol.q: validity = good Process Measured
              UmnATVTR4.Vol.instMag.i: 0
              UmnATVTR4.Vol.q: validity = good Process Measured
            
```

```

0000  01 00 5e 01 01 24 f8 e4 3b e9 73 7b 08 00 45 e0  ..^..$.. ;s{--E-
0010  00 9f f7 49 00 00 20 11 00 00 ac 18 0e 1a ef 01  ..I.....
0020  01 24 e5 34 00 66 00 8b aa f4 01 40 a2 17 80 15  -$-4-f- ...@
0030  00 00 00 72 00 00 00 00 00 02 00 00 00 00 00 0a  .....
0040  00 00 00 01 00 00 00 00 62 82 01 40 00 00 5e 60  .....b-...^
0050  5c 80 01 01 a2 57 30 55 80 04 4d 55 34 39 82 02  \.....wOU ..MU49
0060  00 00 83 04 00 00 00 01 85 01 00 87 40 00 00 00  .....@
0070  00 00 00 00 00 00 01 52 4b 00 00 00 00 ff fe ad  .....R K.....
0080  b5 00 00 00 00 00 00 00 00 00 00 00 00 00 00 00  .....R K.....
0090  00 00 00 00 00 00 01 52 4b 00 00 00 00 ff fe ad  .....R K.....
00a0  b5 00 00 00 00 00 00 00 00 00 00 00 00 00 00 00  .....
    
```

FIGURE 10. R-SV message Wireshark capture.

of fault location is accomplished through ANNs trained with massive amount of three phase voltage and current measurements of all MMG buses and lines during different fault scenarios. A total of 478,980 data patterns were generated to

train and test the neural networks. Data generation and ANN training and testing were performed on MATLAB/Simulink environment for a modified IEEE 14-bus distribution system. The proposed scheme utilizes IEC 61850-based standardized communication to monitor the MMG measurements and send the trip commands. Furthermore, performance evaluation of the proposed protection scheme showed that it is able to accurately detect and locate faults within the MMG. Moreover, the evaluation in terms of end-to-end delays including both ANN computational delay and communication network delay proved compliance of the scheme with IEC 61850-90-5 requirements.

This work can be further extended to consider applying the scheme on another MMG with different configurations and exploring different fault scenarios. Moreover, it is recommended to study the response of the scheme for faults in the Utility Grid when the MMG is operating in grid-connected mode.

REFERENCES

- [1] M. Ghofrani, Ed., *Micro-Grids Applications, Operation, Control and Protection*. London, U.K.: IntechOpen, 2019, doi: [10.5772/intechopen.77550](https://doi.org/10.5772/intechopen.77550).
- [2] S. Beheshtaein, R. Cuzner, M. Savaghebi, and J. M. Guerrero, "Review on microgrids protection," *IET Gener., Transmiss. Distrib.*, vol. 13, no. 6, pp. 743–759, 2019.
- [3] Z. Xu, P. Yang, C. Zheng, Y. Zhang, J. Peng, and Z. Zeng, "Analysis on the organization and development of multi-microgrids," *Renew. Sustain. Energy Rev.*, vol. 81, pp. 2204–2216, Jan. 2018.
- [4] S. M. Brahma, J. Trejo, and J. Stamp, "Insight into microgrid protection," in *Proc. IEEE PES Innov. Smart Grid Technol., Eur.*, Oct. 2014, pp. 1–6.
- [5] A. Srivastava, R. Mohanty, M. A. F. Ghazvini, L. A. Tuan, D. Steen, and O. Carlson, "A review on challenges and solutions in microgrid protection," in *Proc. IEEE Madrid PowerTech*, Jun. 2021, pp. 1–6.
- [6] M. Dewadasa, A. Ghosh, and G. Ledwich, "Protection of microgrids using differential relays," in *Proc. AUPEC*, Sep. 2011, pp. 1–6.
- [7] Z. Alhadrawi, M. N. Abdullah, and H. Mokhlis, "An adjustable differential protection scheme for microgrids with inverter-based distributed generation," *Int. J. Adv. Trends Comput. Sci. Eng.*, vol. 9, nos. 1–4, pp. 664–672, 2020.
- [8] S. Abeid, Y. Hu, F. Alasali, and N. El-Naily, "Innovative optimal nonstandard tripping protection scheme for radial and meshed microgrid systems," *Energies*, vol. 15, no. 14, p. 4980, Jul. 2022.
- [9] T. S. Ustun, C. Ozansoy, and A. Zayegh, "A central microgrid protection system for networks with fault current limiters," in *Proc. 10th Int. Conf. Environ. Electr. Eng.*, May 2011, pp. 1–4.
- [10] A. A. Arani, N. Bayati, G. B. Gharehpetian, R. Mohammadi, and S. H. Sadeghi, "Fault current limiter optimal sizing considering different microgrid operational modes using bat and cuckoo search algorithm," *Arch. Electr. Eng.*, vol. 67, no. 2, Mar. 2018, pp. 321–332.
- [11] H. Lin, K. Sun, Z. Tan, C. Liu, J. M. Guerrero, and J. C. Vasquez, "Adaptive protection combined with machine learning for microgrids," *IET Gener., Transmiss. Distrib.*, vol. 13, no. 6, pp. 770–779, Mar. 2019.
- [12] S. B. Bukhari, "Convolutional neural network-based intelligent protection strategy for Microgrids," *IET Gener., Transmiss. Distrib.*, vol. 14, no. 7, pp. 1177–1185, 2020.
- [13] J. Gu, C. Liu, J. Wang, and M. Yang, "Using IEC 61850 GOOSE messages in microgrid protection," *Int. Trans. Electr. Energy Syst.*, vol. 29, no. 12, Dec. 2019, Art. no. e12122.
- [14] A. A. Memon and K. Kauhaniemi, "An adaptive protection for radial AC microgrid using IEC 61850 communication standard: Algorithm proposal using offline simulations," *Energies*, vol. 13, no. 20, p. 5316, Oct. 2020.
- [15] M. N. Alam, S. Chakrabarti, and A. K. Pradhan, "Protection of networked microgrids using relays with multiple setting groups," *IEEE Trans. Ind. Informat.*, vol. 18, no. 6, pp. 3713–3723, Jun. 2022.
- [16] M. N. Alam, S. Chakrabarti, and X. Liang, "A benchmark test system for networked microgrids," *IEEE Trans. Ind. Informat.*, vol. 16, no. 10, pp. 6217–6230, Oct. 2020.
- [17] M. N. Alam, "Adaptive protection coordination scheme using numerical directional overcurrent relays," *IEEE Trans. Ind. Informat.*, vol. 15, no. 1, pp. 64–73, Jan. 2019.
- [18] J. Bilski, B. Kowalczyk, A. Marchlewska, and J. M. Zurada, "Local Levenberg–Marquardt algorithm for learning feedforward neural networks," *J. Artif. Intell. Soft Comput. Res.*, vol. 10, no. 4, pp. 299–316, Oct. 2020.
- [19] S. Sapna, "Backpropagation learning algorithm based on Levenberg Marquardt algorithm," in *Proc. Comput. Sci. Inf. Technol. (CS&IT)*, 2012, pp. 393–398.
- [20] W. K. A. Najy, H. H. Zeineldin, and W. L. Woon, "Optimal protection coordination for microgrids with grid-connected and islanded capability," *IEEE Trans. Ind. Electron.*, vol. 60, no. 4, pp. 1668–1677, Apr. 2013.
- [21] N. Nimpitiwan, G. T. Heydt, R. Ayyanar, and S. Suryanarayanan, "Fault current contribution from synchronous machine and inverter based distributed generators," *IEEE Trans. Power Del.*, vol. 22, no. 1, pp. 634–641, Jan. 2007.
- [22] H. Margossian, J. Sachau, and G. Deconinck, "Short circuit calculation in networks with a high share of inverter based distributed generation," in *Proc. IEEE 5th Int. Symp. Power Electron. Distrib. Gener. Syst. (PEDG)*, Galway, Ireland, Jun. 2014, pp. 1–5.
- [23] *MATLAB Version: R2023a*, MathWorks, Natick, MA, USA, 2023.
- [24] *NETSIM (Network Simulator)*, Standard 13.2, 2023.
- [25] *INFO TECH*, document 61850 Avenue 2.1, 2023.
- [26] V. D. Andrade and E. Sorrentino, "Typical expected values of the fault resistance in power systems," in *Proc. IEEE/PES Transmiss. Distrib. Conf. Expo., Latin Amer. (T&D-LA)*, Nov. 2010, pp. 602–609.
- [27] M. J. B. B. Davi, D. C. Jorge, and F. V. Lopes, "Fault current and fault voltage analysis of power transmission systems with high penetration of inverter-based wind generators," *Acta Scientiarum. Technol.*, vol. 44, May 2022, Art. no. e57848.
- [28] I. Ali, M. A. Aftab, and S. M. S. Hussain, "Performance comparison of IEC 61850-90-5 and IEEE C37.118.2 based wide area PMU communication networks," *J. Modern Power Syst. Clean Energy*, vol. 4, no. 3, pp. 487–495, Jul. 2016.



ALI F. QUSAYER was born in Madinah, Saudi Arabia, in 1989. He received the B.S. degree in electrical engineering from the King Fahd University of Petroleum and Minerals (KFUPM), in 2011, where he is currently pursuing the M.S. degree. He is an Electrical Engineer with the leading oil company, Saudi Aramco.



S. M. SUHAIL HUSSAIN (Senior Member, IEEE) received the Ph.D. degree in electrical engineering from Jamia Millia Islamia (a Central University), New Delhi, India, in 2018. Currently, he is an Assistant Professor with the Electrical Engineering Department, King Fahd University of Petroleum and Minerals (KFUPM), Dhahran, Saudi Arabia. He is also affiliated with the Interdisciplinary Research Center for Sustainable Energy Systems (IRC-SES) and a fellow with the K.A.CARE Energy Research and Innovation Center (ERIC), KFUPM. Prior to that, he was an AIST Postdoctoral Researcher with the Fukushima Renewable Energy Institute (FREIA), AIST, Koriyama, Japan, and a Senior Research Fellow with the Department of Computer Science, National University of Singapore (NUS), Singapore. His research interests include power system communication, cybersecurity in power systems, and substation automation. He was a recipient of the IEEE Standards Education Grant approved by the IEEE Standards Education Committee for implementing a project and submitting a student application article in 2014–2015. He is an Associate Editor of IEEE OPEN ACCESS JOURNAL OF POWER AND ENERGY.